FAST AND GREEN SYNTHESIS OF Sn/TiO_2 PHOTOCATALYST AND IT'S BI-FUNCTIONAL COMPETENCE AS ADSORBENT AND PHOTOCATALYST

A. MODWI[a,*], B.R Y. ABDULKHAIR[a,b], M. E. SALIH[c], N. Y. ELAMIN[a,d], A. M. FATIMA[a]

[a]*Imam Mohammad Ibn Saud Islamic University (IMSIU), College of Sciences, Department of Chemistry, Riyadh 11623, Saudi Arabia*

[b]*Sudan University of Science and Technology College of Science, Chemistry Department, Khartoum Sudan*

[c]*Shaqra University, College of Science and Humanities, Department of Chemistry-Hurrymila, Shaqra, Saudi Arabia*

[d]*Sudan University of Science and Technology College of Education, Chemistry Department, Khartoum Sudan*

At present, strenuous efforts are being made to enhance the TiO_2 photocatalyst by doping it with Sn. However, there is still scarcity in the reports on the synthesis of a superior TiO_2 photocatalyst in an efficient and simple manner. Therefore, Sn $_{(0\text{-}5\%)}$ doped TiO_2photocatalyst for low-cost photocatalysis and free additive were successfully fabricated through a facile method. The obtained nanomaterials were calcined at 300^oC for 2h and characterized using X-ray diffraction (XRD), Scanning Electron Microscopy (SEM), Fourier Transform Infrared spectroscopy (FTIR), and Energy Dispersive Spectrometer (EDS). The findings demonstrated that, the annealed Sn doped TiO_2 has a good crystallinity and moderated adsorption capacity as well as a superior photocatalysis competence for degradation of Indigo Carmine (IC) dye.

(Received January 24, 2019; Accepted April 18, 2019)

Keywords: Sn/TiO_2 photocatalyst, FTIR, Indigo carmine, Adsorption kinetics, Photodegradation

1. Introduction

Lately, the improve of visible-light-active nanomaterials is in high demand for removal dyes through adsorption and the photocatalysis applications as these nanomaterials can be active either darkness or irradiation. In particular, it is important to develop nanomaterials for the elimination of organic pollutants, existing in a wastewater, which can cause unfavorable effects on human health [1-3].Although customary methods such as UV radiation, ozonation, and separation processes are obtainable to treat organic pollutants, they are expensive and are not environmental. As substitution to these approaches, adsorption and photocatalysis are regarded as a capable process for hazards materials including the adsorption and photodegradation of organic dyes compounds [4-6]. Mostly, wide-bandgap semiconductors such as TiO_2, ZnO, W_2O_3 and SnO_2 are considered as well-organized photocatalysts because of their high redox potential of photocharge carriers [6-9]. Titanium oxide (TiO_2) has been studied comprehensively because of their wide diversity of applications, ranging from gas sensor, hydrogen evolution, and adsorbent to photocatalysis [10-13]. The capability to controller physical characteristics such as crystallinity, specific surface area, pore size, particle size, morphology and method of synthesis resulted in to this huge number of applications. Nowadays, photocatalyst synthesis has gained the focus of the researchers worldwide; the most distinguished being the photocatalyst prepared by doping a semiconductor (metal oxide) with semimetal [14, 15]. Accordingly, the Sn doped TiO_2 nanoparticles have attracted substantial attention because of their broad range of applications arising due to their unique optical and photocatalytic properties [16-19].

* Corresponding author: abuelizkh81@gmail.com

In this work, we demonstrate the influence of the Sn loaded on TiO_2 nanoparticles, which fabricated through simple procedure and calcinated at 300°C for 2h. Addition to the characterization and photocatalysis performance of the fabricated photocatalysts, and it was found that $Sn_{5\%}$doped TiO_2 photocatalyst exhibit an improved markedly.

2. Experimental section

2.1. Materials used

In this paper, Titanium oxide nanoparticles TiO_2 (99.8%) from Sigma-Aldrich, Tin chloride dihydrate $SnCl_2.2H_2O$, was purchased from Merck, was used. Absolute ethanol (99.8%) form Sigma-Aldrich. Indigo Carmine (99.8%) from Loba-Chem was utilized as model of organic pollutant for both, the adsorption and photocatalytic degradation studies. Distilled water was used for preparation purposes. Figure 1, shows the structure of the Indigo Carmine dye.

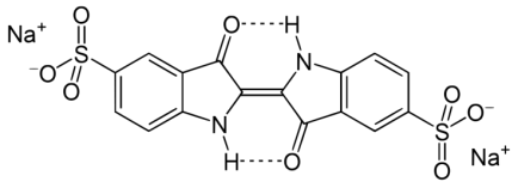

Fig.1. Indigo carmine structure.

2.2. Fabrication of nanomaterials

In the typical procedure, 2 g of titanium oxide (10nm) was dispersed in 3:1 ethanol-water under ultrasonic bath for 10 min. Thereafter, a certain amount of stannous chloride dihydrate (0.1M) were added to the milky titanium oxide suspension under vigorous stirring (650 rpm) and sonicated for further 10 min. Then, the mixtures were heated in dry oven at 90°C for 24 h the powder obtained was also grinded before calcinations. Finally, the white powders were annealed in muffle furnace at 300°C for 2h. The as-prepared Sn-TiO_2 composites with different percentages of Sn species and TiO_2were denoted as x Sn/TiO_2(X = 1.5%, 2.5%, 3.5 and 5%).

2.3. Nanopowder characterizations

The phase purity and crystallinity of the obtained nanomaterials were studied by X-ray diffraction (XRD) and the morphology of all samples was investigated using Scanning Electron Microscopy (SEM). The chemical bonding and vibrations modes of materials were conducted by Fourier Transform Infrared spectroscopy (FTIR) and the elemental composition of prepared nanomaterials was determined through Energy Dispersive Spectrometer (EDS).

2.4. Kinetic adsorption of IC dye procedure

Kinetics adsorption was performed using 100 ml of IC solution with a fixed concentration of 30mg L^{-1}. 50 mg of the composite was added to IC, and stirred for 2hin darkness. A sample was withdrawn at1, 2, 5, 10,15, 30, 60, and 120min, centrifuged, filtered by nylon membrane-syringe filter (0.2µm), and the remained concentration was measured using a spectrophotometer (Labomed – UVS-2800) at a Lambda-max of 611 nm. The quantity of IC adsorbed per gram of nanoparticles at time (min) can be calculated by the following equation (1).

$$q_t = \frac{(C_o - C_t)\times v}{m} \quad (1)$$

where q_t is the adsorbed quantity of IC per gram of IC at time t, C_o is the initial IC concentration, Ct the concentration of IC at time t, v the volume of the solution (mL) and (*m*) the mass of the sorbent used (mg). The data were fitted using the nonlinear Lagergren model for the pseudo-first order (2):

$$q_t = q_e \left(1 - e^{-k\,t}\right) \quad (2)$$

where q_t and q_e is the amount of IC adsorbed at equilibrium, t is time per min, and (k) is the apparent adsorption kinetic constant.

2.5. Photocatalytic degradation procedure

In the typical procedure, 0.05mg of Photocatalyst (TiO_2 and x Sn/TiO_2) agglomerated nanoparticles were dispersed in 100ml of indigo carmine IC (30ppm) in beaker 250ml. Previous to switch light, the mixture was stirred for 50min in the dark to establish the adsorption equilibrium of IC dye on the active side of Photocatalyst. The steady aqueous IC-x Sn/TiO_2 suspension was exposed to UV-visible illumination under continuous stirring. A sample was withdrawn at regular time intervals, centrifuged, filtrated through membrane filter (0.2µ) and the residual concentration was measured. Then the degradation percentage of IC was calculated as follows:

$$Dye\ degradation\ \% = \frac{(C_o - Ct)}{Ct} \times 100 \quad (3)$$

3. Results and discussion

3.1. XRD of Sn loaded on TiO_2nanoparticles

The phase structure and the composition of the fabricated nanomaterials at different Sn contents were characterized employing X-ray diffraction method. The results of XRD patterns for all specimens are presented in (Fig.2.). The peak appearance at 2θ values = 25.22°, 37.7°, 47.9°, 54.0°, 55.0°, 62.5°, 68.7°, 70.2°, 75.1°, were assigned to the (101), (004), (200), (105), (211), (204), (116), (220) and (205) lattice planes of anatase phase of TiO_2 (JCPDS No 89-4921) with high crystallinity [20]. Moreover, the crystallize sizes of all samples were calculated by Debye-Scherer formula [21], and the average crystal size of pure TiO_2 was 8.44nm. For the doped TiO_2 with a different Sn ratio, the average crystallite size of 1.5 Sn / $TiO_2$was increased from 8.44 to 11nm, and it was recognized that the crystallite size was slightly decreased from 11 to 9.6nm by increasing Sn % (Table.1). The tendency of reduction in crystal size became smaller as the ionic radii decreased. The ionic radius of Ti^{4+} (0.605nm) is greatly smaller than that of Sn^{4+} (0.690 nm). Therefore, these relatively large Sn^{4+} ions could be located at the grain junctions and boundaries of the nanoparticles as well as the Ti-O-Sn bonds could be formed, which increased the diffusion barrier and inhibited crystallite growth of TiO_2 anatase [22].

Table 1. XRD parameters of all samples.

Nanomaterials	2Θ	β	Crystallize size (nm)
TiO_2	25.28	0.945	8.4
1.5% Sn/TiO_2	25.25	0.751	11.03
2.5% Sn/TiO_2	25.25	0.771	10.32
3.5% Sn/TiO_2	25.26	0.806	9.88
5% Sn/TiO_2	25.24	0.831	9.58

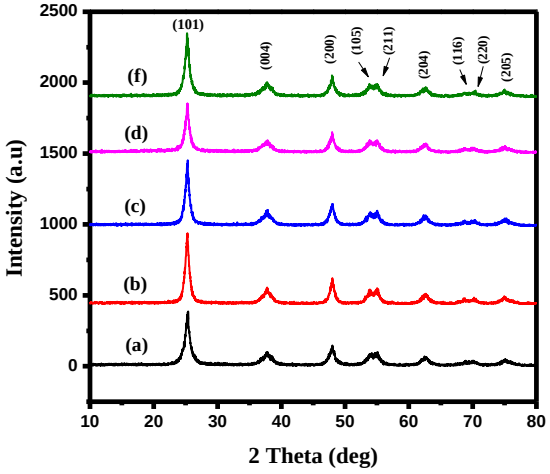

Fig.2. X- Ray Diffraction spectra of (a) TiO_2 , (b) 1.5% Sn/TiO_2, (c) 2.5% Sn/TiO_2 , (d) 3.5% Sn/TiO_2, (f) 5% Sn/TiO_2.

3.2. FTIR studies

The FTIR spectra for the pure, 2.5, and 5-doped TiO_2 photocatalysts are shown in (Fig. 3). The vibration modes at 605 cm^{-1} was assigned to pure O-Ti-O and for 2.5 and 5 Sn decorated TiO_2 nanoparticles was shifted to lower wavenumber from 605 to 586 cm^{-1}. This increment in wavenumber because of the formation Ti-O-Sn bonds [23]. The absorption vibration bands at 1600 cm^{-1} are related with the vibrations of free water molecules, which may be caused by the absorption of moisture during measurements. Consequently, these results proved that the Sn doped TiO_2 nanoparticles were formed with high purity.

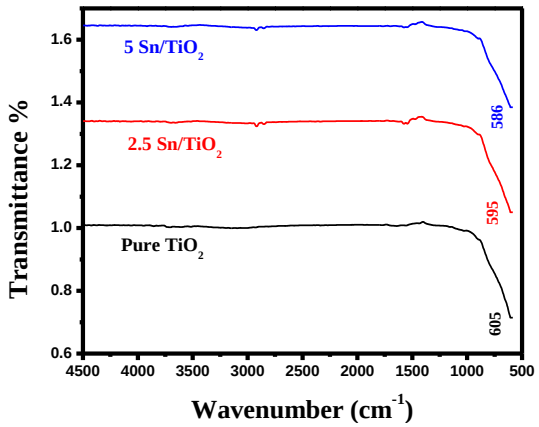

Fig.3. FTIR spectra of (a) pure TiO_2, (b) 2.5 Sn/TiO_2 and (c) 5 Sn/TiO_2.

3.3. SEM and EDAX studies

Fig. 4(a-b) displays undoped and $Sn_{5\%}$doped TiO_2 has irregular spherical shape with small crystallizes size nanoparticles around the range of less than 10 nm. Whereas the 5% Sn doped TiO_2, the agglomeration was decreased and becomes non-uniform of particles shape. To investigate the elements distribution and present in the nanomaterials, the EDX analysis was portrayed and the findings displayed in Fig4(c and d). The spectrum obtained was depicted strong signal at 4.4, 0.5 and 4.5keV corresponding to Ti, O and Sn, respectively. Furthermore, a week signal at 3.4 keV was also observed and it was related to Sn. The EDS mapping was employed to know further about distribution of elements. It can be noticed that, the Sn was homogenous loaded on TiO_2 nanoparticles Fig.4 (f). Therefore, these findings provided evidence that the TiO_2

photocatalyst was successfully loaded by Sn and confirmed the fabrication of Sn/TiO2 nanoparticles.

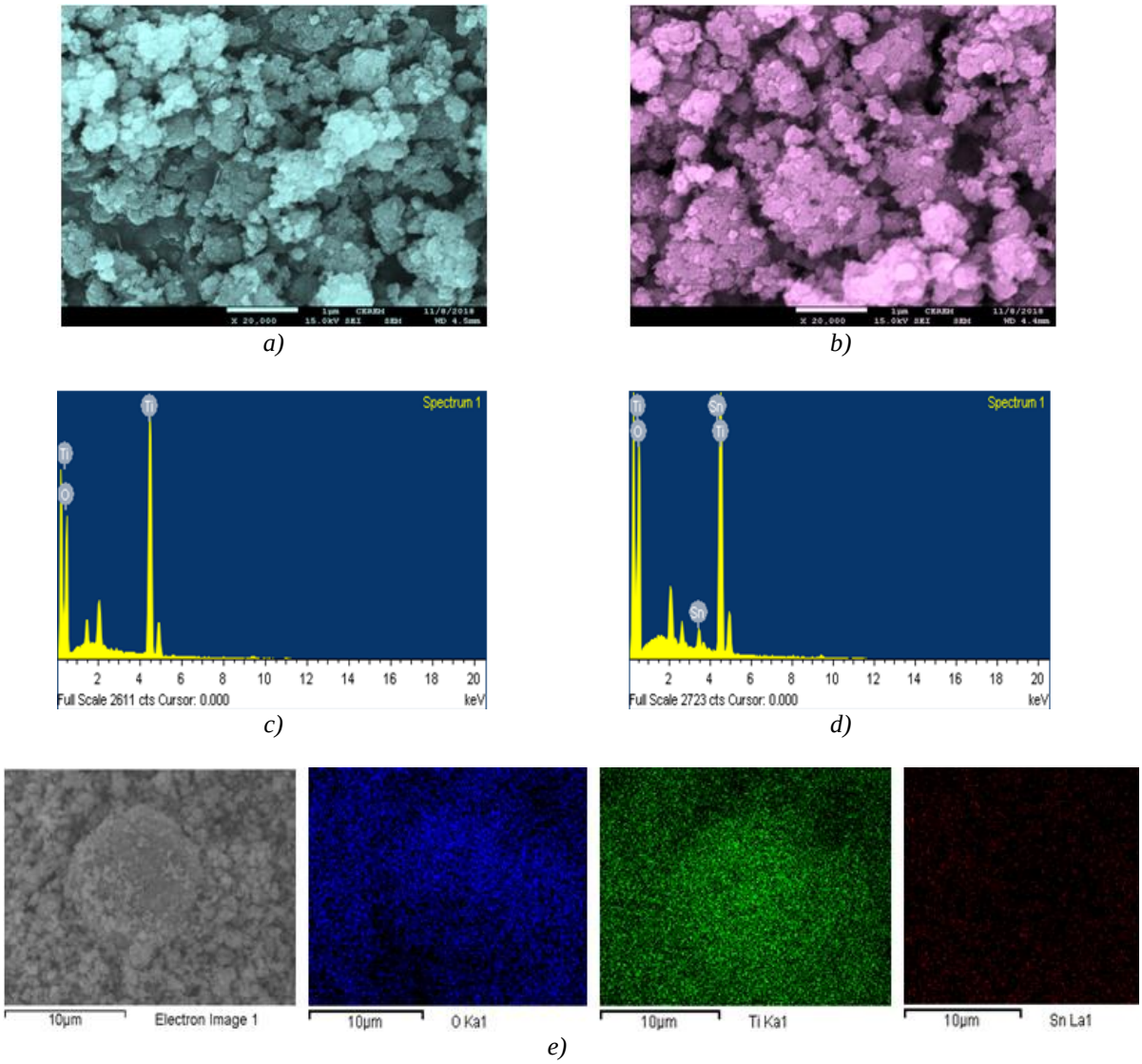

Fig.4. a) SEM images of undoped TiO_2; b) SEM images of 5% Sn doped TiO_2.photocatalyst; c) EDX spectrum of undoped TiO_2; d) EDX spectrum of 5% Sn doped TiO_2 and e) EDX mapping about distribution of Ti, Sn and O elements.

3.4. Determination of the best absorbent and contact time

To assess the adsorption of IC, a series of Sn/TiO_2 nanocomposites were used as adsorbents. It can notice that, apparent increment of Sn from 0 to 5% resulted in increases the adsorption amount of IC. Henceforth, 10 Sn/TiO_2nanocomposite showed higher IC adsorption (66% within 20min) compared to other series Fig. 5(a). Equilibrium contact time is one of most significant parameters affecting the design of contaminated water treatment system. The effect of equilibrium time on IC dye adsorption was demonstrated in Fig.5 (b). It can be noted that, the adsorption was rapid in the early stages of the adsorption process up to it gradually approached an equilibrium. Further increment in contact time does not cause any considerable increase in adsorption competence related to the equilibrium of adsorbent sites [24]. The contact time was less than 50 min in the IC dye concentration of 30 ppm, and short adsorption equilibrium time is useful for the quick adsorption application.

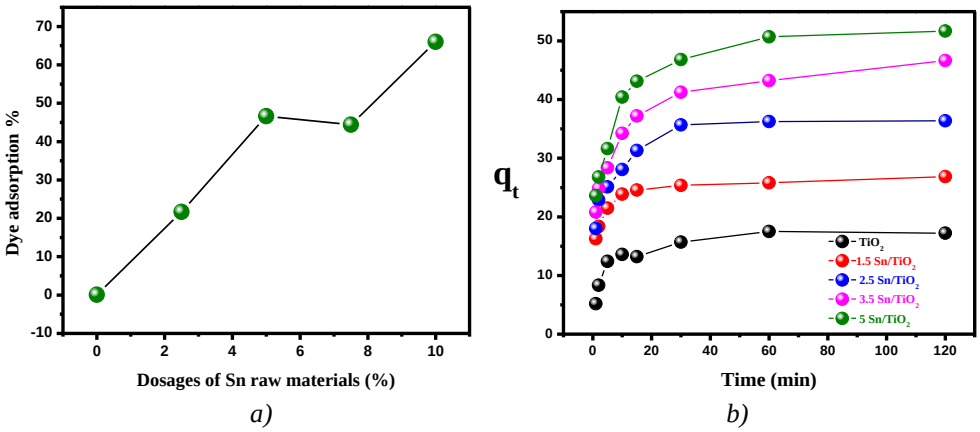

Fig.5. a) the percentage of IC removal on pure and Sn-doped TiO_2 with different Sn raw material; b) Contact time equilibrium.

3.5. Effect of the initial IC concentration

Elimination of organic dyes pollutants by adsorption was extensively utilized to treat wastewaters. In this work, the fabricated Sn/TiO_2nanocomposites are tested as adsorbent for the Indigo carmine (IC). The adsorption equilibrium isotherms can be carried out with 10 mg of the nanocomposites in 25 mL of 10, 30, 50, 70 and 100 mg/L solutions of the IC dye. The solutions with composites were shacked for a 2 h at room temperature. The composites are then separated using centrifuge followed by syringe membrane filter, and the dye concentration in the solution evaluated by spectrophotometer. The obtained data was fitted well with Langmuir model and the removal competency of the dye by the pure TiO_2 and 5 Sn/TiO_2adsorbents were displayed in Fig.6 (a, b) and Table 2.Our results represents a superior sorbents compared to other sorbents announced in the literature, such as: Montmorillonite (40 $mg.g^{-1}$) [25], Chitin nanowhisker (ChNW)-functionalized abrasive spherical materials (0.4 mg g^{-1}) [26], coal fly ash (1.48 mg $.g^{-1}$) [27], zeolite from fly ash(1.23 mg $.g^{-1}$) [28].

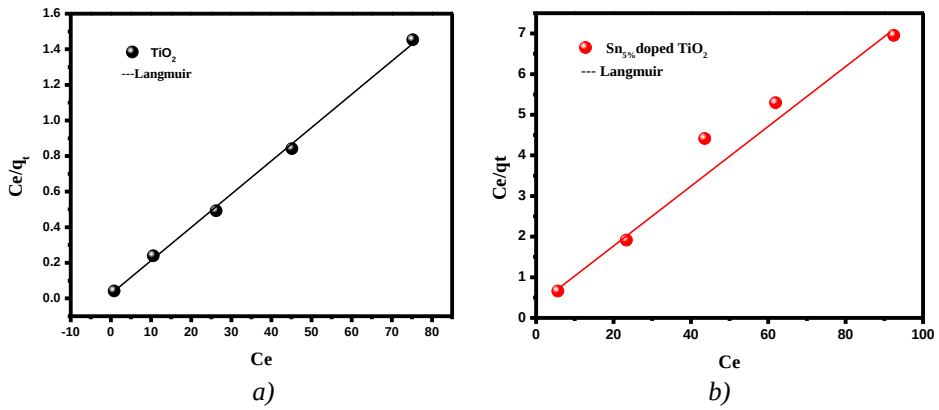

Fig.6. a) Langmuir isothermes of pure TiO_2 ; b) $Sn_{5\%}$ doped TiO_2 adsorbent.

Table 2. Adsorption equilibrium constants for the dye on Pure TiO_2 and 5 Sn/TiO_2 nanoparticles.

Nanomaterials	Langmuir constants		
	q_m(mg.g^{-1})	K_L(l.mg^{-1})	R^2
Pure TiO_2	13.5	0.162	0.967
5 Sn/TiO_2	53.19	0.965	0.998

3.6. Investigation of the photocatalytic performance of the synthesized Sn doped TiO_2 photocatalysts

The photocatalytic properties of the prepared Sn doped TiO_2nanomaterials were evaluated via choosing of IC dye in aqueous solution under UV-visible illumination. The rate of decomposition process of dye was measured by observing the characteristic absorption peak at 611nm and the gradually reduce in the concentration at different time intervals and the results was presented in Fig.7 (a). As can be seen in Fig.7 (b), the photodegradation kinetics of all specimens were well fitted to a pseudo-first order model using the following formula:

$$ln\frac{C_0}{C_t} = kt \tag{4}$$

where *k* is first order rate constant, C_0 initial dye concentration and C_t represent the concentration of solution at time = *t*. The rate degradation constant of pure TiO_2 photocatalyst was found to be equal 16.07 10^{-3} min^{-1} as well as for Sn doped TiO_2 samples were markedly increased with Sn percentage from 15.0210^{-3} min^{-1} to 52.810^{-3} min^{-1}.The increased photocatalytic rate can be attributed to load Sn on the surface of TiO_2 and act as electrons traps resulted in delays recombination [29].Although the obtained results of rate, constants are presented in the Table 3. Besides, it can be clearly noted that, the highest photocatalytic degradation of IC was obtained via $Sn_{5\%}$doped TiO_2 photocatalyst under irradiation. The findings also demonstrated that, the removal percentage of IC after 65 min reaction time was 64.4, 63.3, 69, 76.3 and 96.7% for pure TiO_2, $Sn_{1.5\%}/TiO_2$, $Sn_{2.5\%}$ /TiO_2, $Sn_{3.5\%}$ /TiO_2 and $Sn_{5\%}$ /TiO_2, respectively. Moreover, it is apparent that the percentage degradation of IC is largest with $Sn_{5\%}$ doped TiO_2 photocatalyst as shown in Fig.7(c) and Table 3. These obtained results make $Sn_{5\%}$ doped TiO_2 photocatalyst outstanding catalyst for degradation of IC dye pollutant compared to those announced in the literature [30-32].

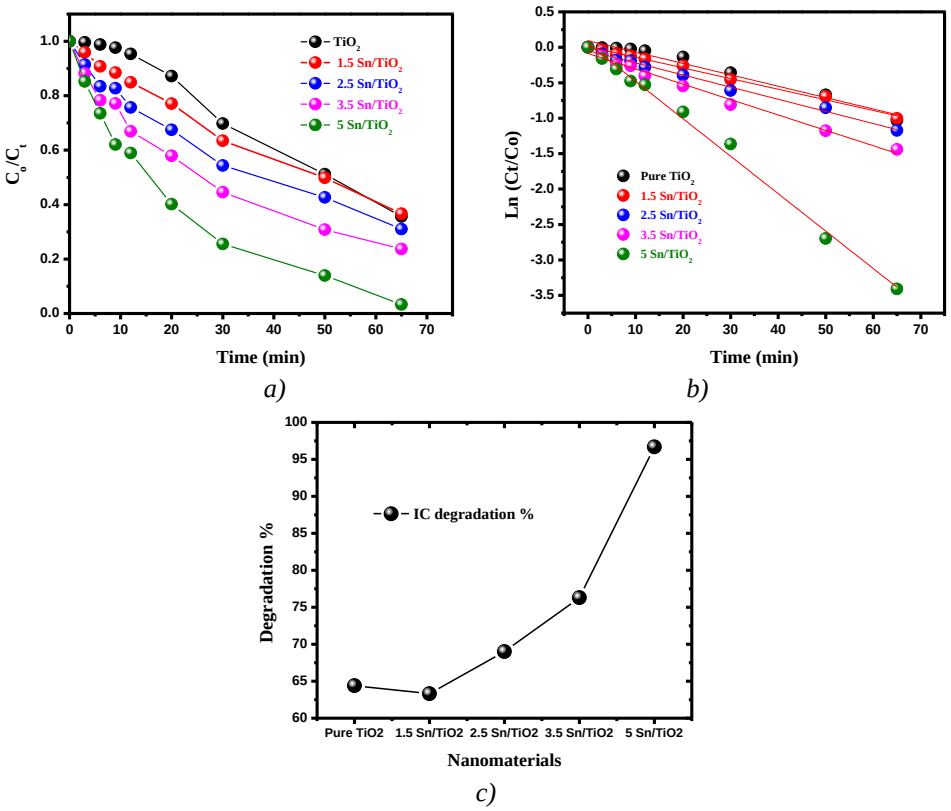

Fig.8.a) Photodegradation of IC using the fabricated samples; b) Rate constant (k) for the degradation of IC; c) Photocatalysis percentage efficiency.

Table 3. Rate constant and IC dye degradation efficiency of photocatalysts.

Photocatalyst	TiO_2	1.5 Sn/TiO_2	2.5 Sn/TiO_2	3.5 Sn/TiO_2	5 Sn/TiO_2
Pseudo first order constant (10^{-3} min^{-1})	16.07	15.02	17.14	21.7	52.8
Degradation efficiency %	64.4	63.3	69	76.3	96.7
R^2	0.975	0.994	0.991	0.987	0.993

4. Conclusions

To recapitulate of this work, x Sn/TiO_2nanoparticleswith splendid photocatalysis property were successfully fabricated by simplistic and free additive method. The TiO_2nanoparticles were dispersed in ethanol-water until milky solution formed and followed by spiking with required amount of Sn solution and the powder obtained was calcined at 300 ^oC for 2 h. The effect of adsorption parameters such as IC, contact time, initial concentration was estimated.

The findings demonstrated that the adsorption time was fast and reaching equilibrium within 40 min and Langmuir isotherm with a maximum adsorption capacity of 53.12 mg. g^{-1}. The photocatalytic degradation of IC dye was investigated and $Sn_{5\%}$doped TiO_2 nanomaterials was exhibited superior photocatalyst. Furthermore, the fabricated photocatalyst (Sn/TiO_2) is proposed to be magnificent candidates as photocatalyst for organic pollutants in industrial wastewater.

References

[1] C. Teerapatsakul et al., International Biodeterioration & Biodegradation **120**, 52 (2017).
[2] E. Forgacs, T. Cserhati, G. Oros, Environment international**30**(7), 953 (2004).
[3] K.-T. Chung, C.E. Cerniglia, Mutation Research/Reviews in Genetic Toxicology**277**(3), 201 (1992).
[4] B. Mohamed et al., Preparation and characterization of homoionic montmorillonite modified with ionic liquid: Application in dye adsorption. Colloids and surfaces, 2018.
[5] Y. Zhang et al., Solar Energy **173**, 993 (2018).
[6] R. Qian et al., Charge Carrier Trapping, Recombination and Transfer during TiO2 Photocatalysis: An Overview. Catalysis Today, 2018.
[7] P. Dash et al., Synthesis and characterization of aligned ZnO nanorods for visible light photocatalysis. Physica E: Low-dimensional Systems and Nanostructures, 2018.
[8] M. T. Zahoor et al., Materials Chemistry and Physics **221**, 250 (2019).
[9] A. Kusior et al., Journal of the European Ceramic Society **33**(12), 2285 (2013).
[10] M. Rieu et al., Procedia engineering **120**, 75 (2015).
[11] R. Shwetharani et al., Materials Letters **218**, 262 (2018).
[12] M. Pazoki,M. Parsa, R. Farhadpour, Journal of Environmental Chemical Engineering**4**(4), 4426 (2016).
[13] M. Stucchi et al., Ultrasonics sonochemistry **44**, 272 (2018).
[14] G. Sanzone et al., Superlattices and Microstructures **123**, 394 (2018).
[15] D. Sánchez-Rodríguez et al., Journal of Environmental Chemical Engineering **6**(2), 1601 (2018).
[16] Q. Cai et al., Electrochimica Acta **261**, 227 (2018).
[17] J. Li et al., Journal of Alloys and Compounds **679**, 454 (2016).
[18] X. Li, R. Xiong, G. Wei, Journal of Hazardous materials **164**(2-3), 587 (2009).
[19] A.K. Tripathi et al., Journal of Alloys and Compounds **622**, 37 (2015).
[20] S. Mehraz et al., Large scale and facile synthesis of Sn doped TiO2 aggregates using hydrothermal synthesis. Solar Energy Materials and Solar Cells, 2017.
[21] A. Modwi et al., Journal of Materials Science: Materials in Electronics **27**(12), 12974 (2016).
[22] F. Zhou et al., Fabrication and characterization of TiO 2/Sepiolite nanocomposites doped with rare earth ions. Materials Letters, 2018.

[23] F.-X. Xiao, ACS applied materials & interfaces **4**(12), 7055 (2012).
[24] A. Meng et al., ACS applied materials & interfaces **7**(49), 27449 (2015).
[25] F. Geyikçi, Progress in Organic Coatings **98**, 28 (2016).
[26] C. N. Arenas et al., Process Safety and Environmental Protection **106**, 224 (2017).
[27] T. de Carvalho et al., Journal of Radioanalytical and Nuclear Chemistry **289**(2), 617 (2011).
[28] M. Ahmed, A. Mohamed, Chemosphere **174**, 280 (2017).
[29] A. Barmeh, M.R. Nilforoushan, S. Otroj, Thin Solid Films **666**, 137 (2018).
[30] S. Sood et al., Journal of Alloys and Compounds **650**, 193 (2015).
[31] K. D. Lakshmi et al., Visible Light Driven Mesoporous Mn and S Co-doped TiO2 Nano material: characterization and Applications in Photocatalytic Degradation of Indigocarmine dye and Antibacterial Activity. Environmental Nanotechnology, Monitoring & Management, 2018.
[32] S. L. Mora et al., Industrial Crops and Products**126**, 302 (2018).